Journal of Alloys and Compounds 506 (2010) 666–672

Contents lists available at ScienceDirect

Journal of Alloys and Compounds

journal homepage: www.elsevier.com/locate/jallcom

Catalyst-free combined synthesis of Zn/ZnO core/shell hollow microspheres and metallic Zn microparticles by thermal evaporation and condensation route

Waheed S. Khan, Chuanbao Cao*, Ghulam Nabi, Ruimin Yao, Sajjad H. Bhatti

Research Centre of Materials Science, Beijing Institute of Technology, Beijing 100081, People's Republic of China

ARTICLE INFO

Article history:
Received 5 February 2010
Received in revised form 7 July 2010
Accepted 7 July 2010
Available online 15 July 2010

Keywords:
Metal-semiconductor
Core/shell microstructure
Thermal evaporation and condensation
Optical properties

ABSTRACT

Here we report catalyst-free combined synthesis of metal/semiconductor Zn/ZnO core/shell microspheres with hollow interiors on Si substrate and metallic Zn polygonal microparticles on glass substrate in a single experiment via thermal evaporation and condensation technique using nitrogen (N_2) as carrier agent at 800 °C for 120 min. The Zn/ZnO hollow microspheres were observed to have dimensions in the range of 70–80 μm whereas metallic Zn microparticles with polygonal cross section and oblate spherical shape were found to be of 8–10 μm. Some of the Zn/ZnO core/shell hollow spheres were also observed to have single crystalline ZnO pointed rods in extremely low density grown on the outer shell. The structural, compositional and morphological characterization of the products obtained on the substrates were performed by X-ray diffraction (XRD), energy dispersive X-ray spectroscopy (EDS), scanning electron microscopy (SEM), transmission electron microscopy (TEM) and selected area electron diffraction (SAED). A vapor–liquid–solid (VLS) process based growth mechanism was proposed for the formation of Zn/ZnO core/shell microspheres with hollow interior. The optical properties of Zn/ZnO core/shell microspheres were investigated by measuring the photoluminescence (PL) spectra at room temperature (RT). Two very strong emission bands were observed at 373 and 469 nm in the ultraviolet and visible regions respectively under excitation wavelength of 325 nm. Also the effect of the various excitation wavelengths on the PL behaviour was studied at room temperature. PL studies of Zn/ZnO core/shell microspheres show the promise of the material for applications in UV and blue light optical devices.

1. Introduction

During the past few years, micro- and nanoscale composite materials with core/shell structure have stimulated tremendous research interest owing to their fascinating properties like small size, large surface area, quantum dimension and their useful applications in photocatalysis, optoelectronics, magnetics, biology and lithium-ion batteries [1–5]. Among numerous other useful composite materials, Zn/ZnO core/shell structures are of special interest because of the heterojunctions established at the interface of the composite material. A latest research has revealed the room temperature ferromagnetism in Zn/ZnO core–shell structure attributed to the point defects in the interface region of Zn/ZnO heterostructure. These results not only indicate the potential applications of Zn/ZnO core–shell structures in spintronics but also may be helpful for understanding the origin of ferromagnetism in undoped ZnO [6]. The heterojunctions resulting from ZnO (semiconductor) and Zn (metal), which have big contrast in many characteristics, offer great promise for fabricating various devices with improved features like enhanced optical emission [7], field emission [8], solar energy conversion [9] and application in nanotransducers [10], optoelectronic nanodevice [11] and micro- and nano-electromechanical devices [12]. Many reports have been published in literature regarding the formation of metal/semiconductor Zn/ZnO core/shell structures with various morphologies like chestnut-like Zn–ZnO hollow nanostructures [13], urchin-like Zn/ZnO core–shell structures [9], hierarchical Zn/ZnO structures [8], Zn/ZnO core–shell nanoparticles [14], Zn/ZnO treelike nanostructures [7] and Zn/ZnO core–shell nanorods [15], etc. Among these Zn/ZnO based core/shell structures, microspheres with hollow interior are of high technological importance owing to their appealing features, for example low density, high surface area, good permeation and distinct optical properties [16–18]. Different preparative methods have been reported regarding the synthesis of Zn/ZnO core/shell microspheres such as direct thermal oxidation process using Zn as a source material [19], hydrothermal synthesis of Zn/ZnO core/shell microspheres [20] and chemical vapor deposition (CVD) strategy to obtain hollow-opened ZnO/Zn or solid Zn/ZnO microspheres on Si substrate using high purity Zn and ZnO powder as sources [21], etc.

In large number of reports on ZnO nano- and microstructures such as nanowires, nanorods, nanotubes, spheres, polyhedrons and

* Corresponding author. Tel.: +86 10 6891 3792; fax: +86 10 6891 2001.
E-mail address: cbcao@bit.edu.cn (C. Cao).

0925-8388/$ – see front matter © 2010 Elsevier B.V. All rights reserved.
doi:10.1016/j.jallcom.2010.07.039

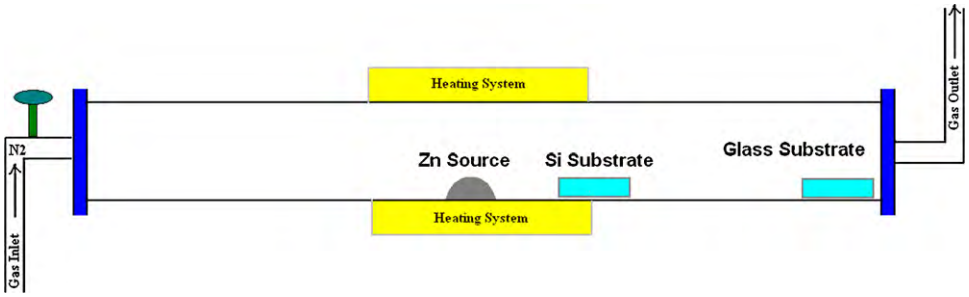

Fig. 1. Schematic diagram for the experimental setup of Zn/ZnO core/shell hollow microspheres and Zn microparticles at 800 °C under N_2 flow.

cages, catalyst-assisted vapor–liquid–solid (VLS) growth process has been employed [22,23]. In this approach, catalyst particle plays crucial role for establishing favourable site to help the landing of condensing species and growing the structures. Although VLS growth has been widely used and is very powerful technique for the preparation of well-oriented nanostructures but it requires quite hard conditions like high temperature, use of some catalyst or additive and complicated atmosphere [24]. Some other drawbacks of this route are the incorporation of catalyst particles as contamination in the final product which creates deep-level traps and defects affecting the device performance [25]. In contrast, catalyst-free growth technique does not demand any tough conditions and is considered very simple, attractive, inexpensive as well as free of defects [26].

In this research, Zn/ZnO core/shell microspheres with hollow interior and metallic Zn solid microparticles were simultaneously synthesized respectively on Si and glass substrates under N_2 flow by thermal evaporation and condensation route. SEM images showed the average diameter of the Zn/ZnO microspheres as 70–80 μm and that of Zn solid microparticles as 8–10 μm. Some of Zn/ZnO hollow spheres were also observed with ZnO pointed rods in quite low density on outer shell. A four step VLS growth mechanism was proposed for the formation of Zn/ZnO core/shell microspheres with hollow interiors and small open holes on the shell. Room temperature PL spectrum exhibited a strong ultraviolet (UV) emission at 373 nm and an intensive and broad blue emission at 469 nm. This shows that Zn/ZnO core/shell hollow microspheres have potential applications in UV and blue light emitting devices.

2. Experimental

One glass and one Si substrate ultrasonically cleaned in ethanol and rinsed with de-ionized water were placed in the downstream zone at different distances from the source inside alumina tube mounted in the horizontal tube (HT) furnace. The Si substrate was placed at about 10 cm from the central position of the furnace whereas the glass substrate was positioned just close to the downstream end of the furnace as shown in schematic diagram of Fig. 1. About 1 g zinc powder (99.9% STREM Chemicals, USA) was loaded in a semicircular long alumina boat and shifted to the center of alumina tube (with 100 cm length and 2.5 cm diameter) fitted in the horizontal tube (HT) furnace. After sealing HT furnace tightly from both ends, it was pumped out using a mechanical rotatory pump for removing the residual air contents from the furnace tube and then also flushed heavily with high purity nitrogen (N_2) gas for about 5 min. Later on N_2 gas flow was adjusted at 150 sccm (standard cubic centimeter per minute) and the furnace was switched on to reach the target temperature of 800 °C at ramp rate of 10 °C/min. 800 °C was maintained for a reaction time of 120 min and then furnace was cooled down naturally. A dark gray color product was obtained on Si substrate whereas gray color easily removable powder was obtained on glass substrate and preserved in airtight plastic bag for further investigations.

The structure and the phase purity of the products on Si and glass substrates were determined by X-ray powder diffraction (XRD, Philips X'Pert Pro MPD) with Cu Kα radiation (λ = 0.15406 nm) whereas the morphologies of the products were examined by scanning electron microscopy (SEM, Hitachi S-3500). The chemical composition of the product was tested by EDS. PL characteristics were studied at room temperature by using Hitachi FL-4500 spectrofluorometer.

3. Results and discussion

3.1. Structural characterization

Fig. 2 shows the X-ray diffraction (XRD) spectrum of the dark-gray color product obtained on Si substrate after heating zinc powder at 800 °C under N_2 flow for 120 min. All diffraction peaks in the spectrum can be indexed to hexagonal Zn and wurtzite ZnO. The lattice parameters calculated for Zn are $a = 0.2668$ nm and $c = 0.4952$ nm which are very close to the standard values of JCPDS Cards No. 004-0831 for Zn. Similarly for ZnO, $a = 0.3252$ nm and $c = 0.5206$ nm are in agreement with JCPDS Cards No. 013-1451. The strongest peak in the spectrum positioned at $2\theta = 69.10°$ belongs to Si owing to Si substrate. The high crystallinity of the as-grown sample is indicated by the sharpness of the diffraction peaks. All diffraction peaks are accounted for Zn and ZnO and no impurity phase like Zn_3N_2 is present in the product.

Fig. 3 shows typical SEM images of Zn/ZnO core–shell hollow microspheres obtained on Si substrate. From low magnification SEM image (a), it can be seen that a large number of hollow microspheres are distributed on the surface of Si substrate. The open holes with various size and different shapes on the surface of the microspheres reveal their hollow nature. The average diameter of the hollow spheres is in the range of 70–80 μm whereas thickness of the shell ranges from 200 to 250 nm as depicted in the magnified images (b–d). The interior portion of the microspheres is highly fine and smooth whereas exterior one is quite rough due to ZnO nanoislands formed on the outer surface. On some of the hollow microspheres, these nanoislands have grown into long single crys-

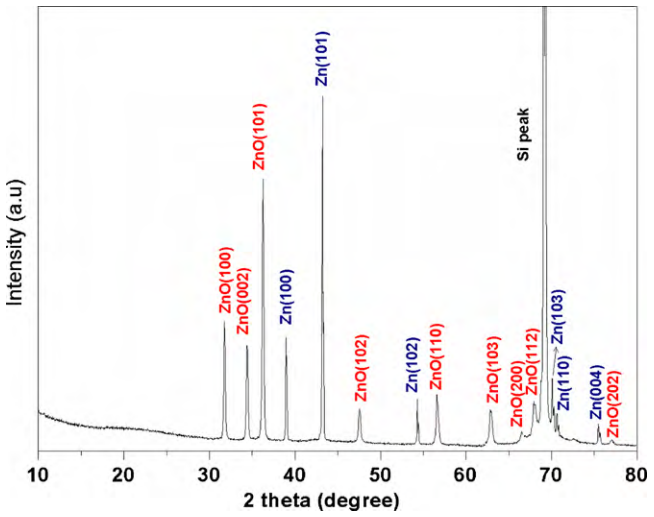

Fig. 2. XRD spectrum of Zn/ZnO core/shell hollow microspheres synthesized on Si substrate.

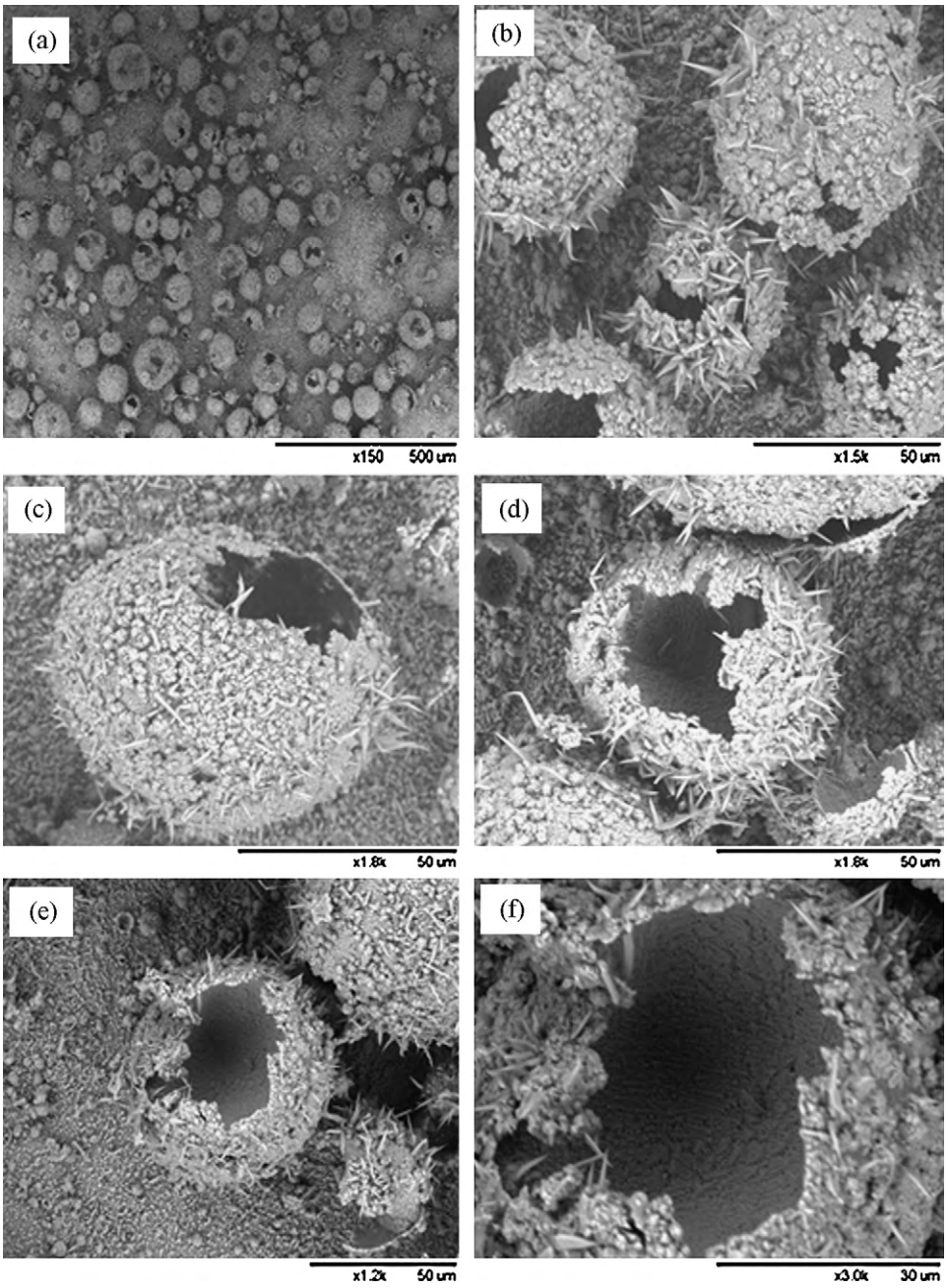

Fig. 3. (a) Low magnification SEM micrographs of Zn/ZnO core/shell microspheres on Si substrate. (b)–(d) Magnified SEM images of Zn/ZnO core–shell microspheres with hollow interiors and with low density of ZnO rods grown on shell.(e) and (f) SEM images showing smooth interior surface and highly rough outer surface.

talline ZnO pointed rods but the density of the rod-like structures is extremely low as compared with rods on Zn/ZnO core/shell microcactuses obtained under ammonia at 600 °C reported elsewhere [27]. Some contrast between inner and outer portion of the microsphere is also evident from image (f). Inner surface seems to be dark as compared to outer surface which is possibly due to the presence of zinc in the inner side which had not oxidized in the process. The light color of outer shell is due to ZnO layer.

Fig. 4a shows a TEM image measured from single ZnO rod grown on microspheres. The rod does not have uniform cross sectional area along its length but it seems like a solid cone. The diameter of the rod gradually decreases from stem (thick end) towards sharply pointed tip part which is consistent with the SEM results. The SAED pattern in the inset of Fig. 4a confirms the single crystal nature of the as grown ZnO rod. EDS spectrum of the as-synthesized Zn/ZnO core/shell microspheres is displayed in Fig. 4b. It shows that core/shell microspheres are composed of Zn (core) and ZnO (shell). The Si peak in the EDS spectrum is due to the Si substrate and no phase impurity is observed in the product.

3.2. Growth mechanism

Based on the evidences obtained from experimental results and characterization analyses, we propose a growth mechanism for the formation of Zn/ZnO core/shell hollow microspheres elaborated in four steps and illustrated in Fig. 5. These four steps include vaporization and condensation of zinc on Si substrate; nucleation of Zn droplets into zinc microspheres; formation of ZnO layer and some rod-like structures through oxidation of zinc on the outer surface and finally sublimation of zinc from interior of microspheres causing hollow interior. The detailed description of the growth mechanism can be given as below.

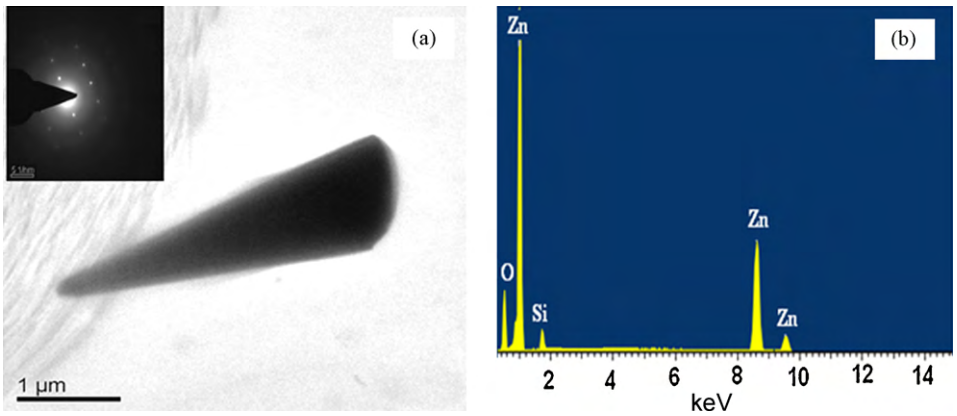

Fig. 4. (a) TEM image of ZnO pointed rod whereas inset exhibits its SAED pattern. (b) EDS spectrum of Zn/ZnO core/shell microspheres.

Firstly, when zinc powder is heated in N_2 gas environment inside horizontal tube furnace, it melts at 419 °C (melting point of Zn) and further heating converts it into vapors due to vapor–liquid equilibrium.

$$Zn(s) \rightarrow Zn(v) \quad (1)$$

Due to nitrogen gas flow and concentration diffusion [10], these Zn vapors are transported downstream towards the comparatively low-temperature region and condense on the surface of Si substrate. Secondly, the condensing Zn vapors convert into droplets and nucleate into the micro-sized zinc spheres. Thirdly, under increased temperature conditions at the center of the furnace, the temperature at the deposition region also increases. In such enhanced temperature environment, the residual and/or leaky oxygen plays its role to react with the zinc on the outer surface of Zn microspheres to form ZnO nuclei

$$2Zn + O_2 \rightarrow 2ZnO \quad (2)$$

Other possible source of oxygen inclusion in the system may be the impurities of nitrogen used; oxygen atoms in quartz (SiO_2) reaction tube [28] or alumina (Al_2O_3) reaction boat or tube [29]. At the same time, Zn vapors in equilibrium with liquid Zn, also react with oxygen, and deposit on the shells due to the absorption by the ZnO particles in the shell. As a result, ZnO layer gradually becomes thick on the outer surface of the spheres. On the exterior part of the spheres, ZnO nuclei nucleate to form nanoislands resulting in the rough outer surface. These nanoislands become favourable sites for upcoming ZnO species on some spheres and grow into rod-like structures emerging out of the shell. When the temperature at the center of the furnace tube reaches 800 °C and is maintained for 120 min, then due to temperature gradient the temperature at Si substrate location is about 750–760 °C. Finally, at such high T conditions at Si substrate position, the liquid Zn at the core of the microsphere evaporates and exerts vapor pressure on the inner side of the shell. This causes the shell breakage and consequently zinc vapors diffuse out of broken part [30]. Further oxidation of outer shell of the ZnO structures prevents the Zn vapor diffusion maintaining Zn layer inside. Therefore, the sphere's shell consists of ZnO layer and the metal Zn (core) on the inner-shell does not oxidize completely, which is in agreement with XRD and SEM observations.

It is worth-mentioning that while heating the Zn powder, temperature ramping stage (RT to 800 °C) is quite crucial for zinc

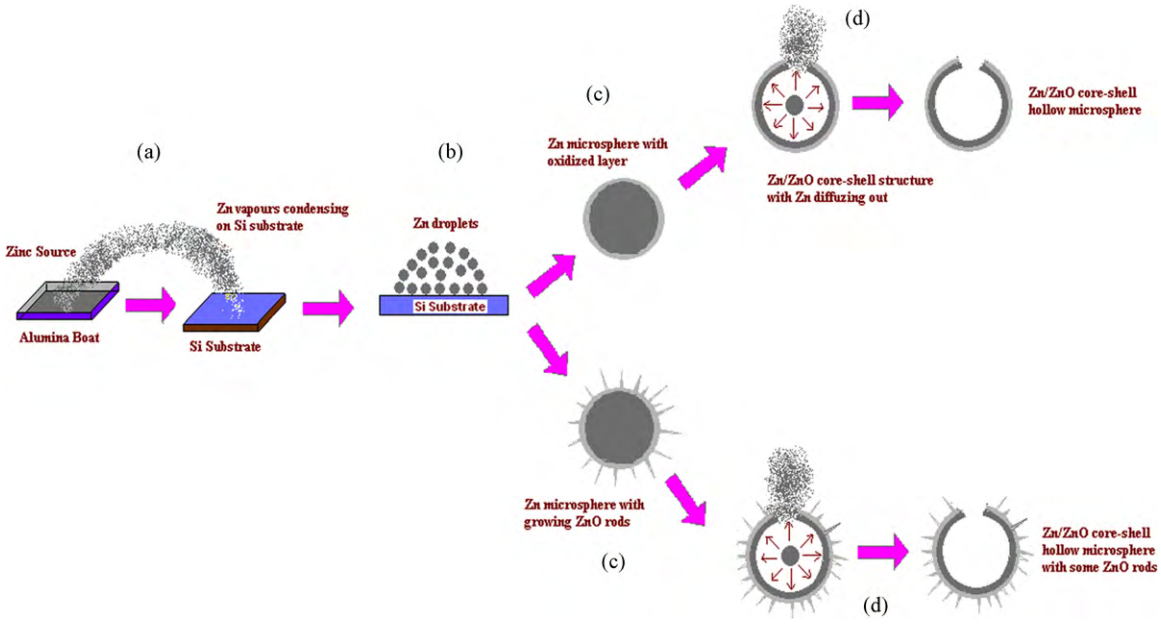

Fig. 5. Growth mechanism for the formation of Zn/ZnO core/shell hollow microspheres. (a) Zinc powder evaporates on heating and then condenses on Si substrate. (b) Nucleation of Zn droplets into zinc microparticles. (c) Formation of ZnO layer and some rod-like structures through oxidation of zinc on the outer surface. (d) Sublimation of zinc from interior of microspheres causing hollowness.

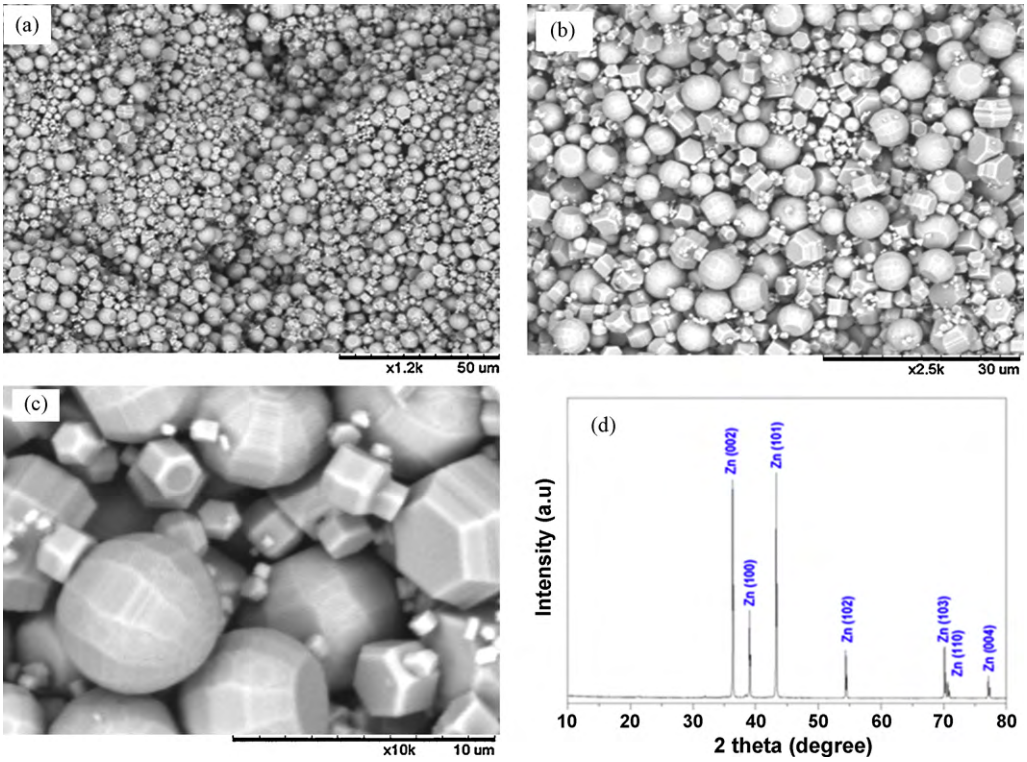

Fig. 6. (a) Low and (b) medium magnification SEM micrographs exhibiting Zn metal microparticles. (c) High magnification SEM image of Zn metal microparticles giving the close look of microparticles. (d) XRD spectrum of metallic Zn microparticles obtained on glass substrate.

deposition on Si substrate whereas steady temperature stage maintained for 120 min is important for zinc vapors to be deposited on the furnace tube walls and also on glass substrate placed at low T zone near downstream end. No source material was found left in the reaction boat after cooling the furnace to room temperature. As there was small temperature gradient at Si position, so zinc was also oxidized at the outer layer. But the temperature of downstream end near glass substrate position was very low about 200–250 °C, so the chances of the oxidation of zinc product were quite feeble. That is why pure metallic Zn microparticles were obtained on glass substrate.

Fig. 6 shows the SEM micrographs of the zinc metal product obtained on the glass substrate placed at the downstream end of HT furnace. It can be clearly seen in low (a) and medium magnification (b) SEM images that there are a large number of particles which are seemingly sphere-like. The particles are not same either in size or shape. Some are very large in size and other are much smaller. The high magnification SEM image (c) reveals that powder product deposited on glass substrate consists of large and small microparticles. The large size particles are of oblate spherical shape with flat polygonal cross-sectional surface whereas small particles have hexagonal cylindrical shape. The morphology of these particles is different from that obtained under ammonia gas at 800 °C [31] where microparticles with high uniformity had a layered oblate spherical structure with hexagonal cross-section. The size of the large microparticles lies in the range of 8–10 μm whereas smaller particle have dimensions in the range of 2–3 μm. The XRD spectrum of the product obtained on glass substrate is depicted in Fig. 6d. All diffraction peaks in the spectrum can be indexed to hexagonal Zn. The lattice parameters calculated for Zn were found to be in agreement with JCPDS Cards No. 004-0831. No other phase like ZnO or Zn_3N_2 is observed in the product.

EDS spectrum of the product obtained on glass substrate is displayed in Fig. 7a. It shows that microparticles are composed of Zn.

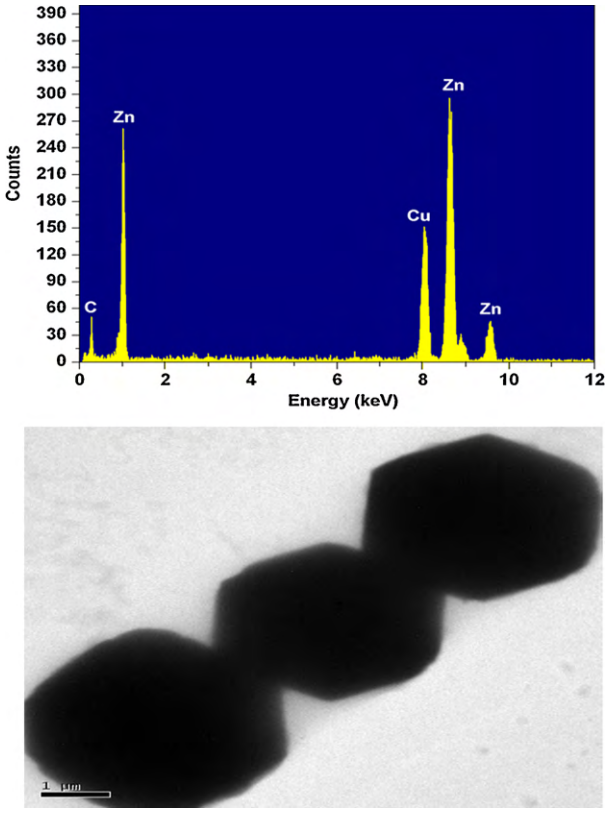

Fig. 7. (a) EDS spectrum of Zn microparticles obtained on glass substrate. (b) TEM image of polygonal Zn microparticles exhibiting solid interior.

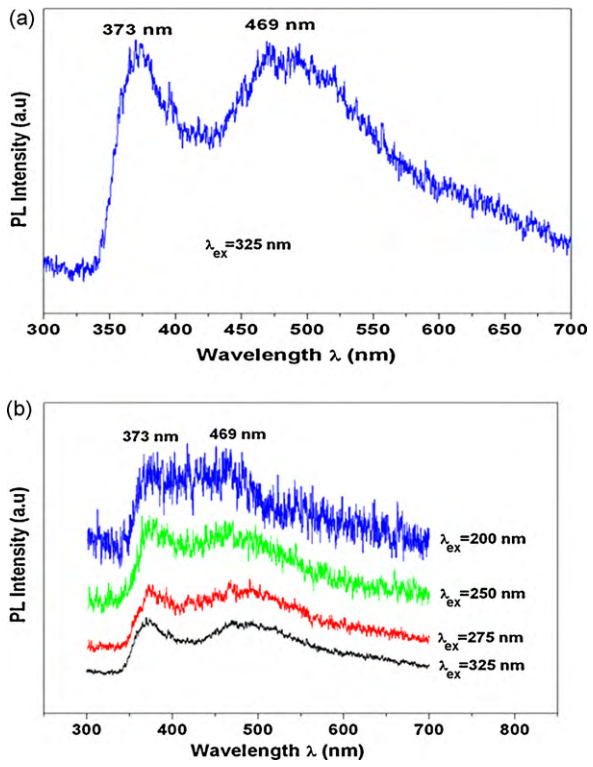

Fig. 8. (a) Room temperature PL spectrum of Zn/ZnO core/shell hollow microspheres at λ_{ex} = 325 nm. (b) PL spectra at four different excitation wavelengths.

Peaks of copper (Cu) and carbon (C) appeared in the spectrum are due to copper grid and carbon coating. No other element is present in the obtained product. Fig. 7b shows a TEM image of Zn microparticles. It shows the polygonal cross-section of the zinc particles with solid interior.

3.3. PL properties

Room temperature photoluminescence (PL) spectrum of Zn/ZnO core/shell hollow microspheres synthesized at 800 °C under nitrogen gas flow is depicted in Fig. 8a. The spectrum has been obtained by using xenon lamp at an excitation wavelength of 325 nm. Two very strong and dominating emission bands can be observed in the PL spectrum: an ultraviolet (UV) band centered at 373 nm (3.33 eV) and a blue band centered around 469 nm (2.64 eV).

The UV emission band slightly dominating the blue emission (BE) in the PL spectrum corresponds to near-band edge (NBE) emission of ZnO [32] and is generally attributed to direct recombination of an electron in conduction band with a hole in valence band [33]. BE bands have also been observed for Zn/ZnO core/shell structures at 452 and 441 nm along with UV emissions at 370 and 374 nm, respectively [7,26]. But these blue emissions are quite scarce compared with green and yellow emission from Zn/ZnO structures which have been reported at large [10,19,21,34,35]. The deep-level emissions in the visible region exhibited by the hollow Zn/ZnO structures are generally ascribed to the defects in the ZnO lattice such as oxygen vacancy V_o, zinc vacancy V_{Zn}, interstitial zinc (Zn_i), etc. that are due to both lattice mismatch (Zn/ZnO) and incomplete oxidation of Zn [34,36–38]. Sun [39] worked out the energy level values of the intrinsic defects in undoped ZnO films, such as oxygen vacancy (V_o), zinc vacancy (V_{Zn}), interstitial oxygen (O_i), interstitial zinc (Zn_i), and antisite oxygen (O_{Zn}) using full-potential linear muffin-tin orbital method. The BE peak at 2.64 eV (469 nm) is smaller than band gap of ZnO (3.37 eV) which indicates that blue emission is related with local defects. The value of energy interval from shallow Zn_i level to the top of the valence band is about 2.90 eV [39] which is quite close to the blue emission of 2.64 eV (469 nm) observed in the present case. The low formation energy of Zn_i shallow donors also enhances their formation probability [40]. The energy interval between the bottom of the conduction band and V_{Zn} level (3.06 eV) is also somewhat closer to the blue emission. But the probability of forming V_{Zn} is less than that of Zn_i owing to larger enthalpy of defect (ΔH). The value of ΔH for V_{Zn} is 7.0 eV whereas for Zn_i, ΔH is 4.0 eV [39]. The oxygen vacancy defects V_o cannot be associated with the blue emission because the energy interval between conduction band and V_o is 1.62 eV which is too small. Therefore, we can attribute blue PL emission at 469 nm only to zinc interstitial (Zn_i) like defects.

The effect of excitation wavelength on the PL characteristics has also been investigated at room temperature. The product was excited by xenon light source at excitation wavelength values of 200, 250, 275 and 325 nm and corresponding effect has been depicted in the Fig. 8b. No shift of emission bands was observed upon the variation of wavelength but only PL emission intensity was found to be enhanced with decreasing excitation wavelength which is an obvious result.

4. Conclusions

In conclusion, Zn/ZnO core/shell microspheres with hollow interior and Zn microparticles were simultaneously synthesized respectively on Si and glass substrates under N_2 flow by thermal evaporation and deposition route. SEM images showed that the average diameters of Zn/ZnO hollow microspheres and metallic Zn microparticles are in the range of 70–80 μm and 8–10 μm, respectively. Some of Zn/ZnO hollow spheres were also observed with single crystalline ZnO pointed rods in quite low density on outer shell. A four step VLS growth mechanism was proposed for the formation of Zn/ZnO core/shell microspheres with hollow interiors and small open holes on the shell. Room temperature PL spectrum exhibited a strong ultraviolet (UV) emission band at 373 nm and an intensive and broad blue emission at 469 nm. This shows that Zn/ZnO core/shell hollow microspheres have potential applications in UV and blue light emitting devices.

Acknowledgement

This work was supported by National Natural Science Foundation of China (Grant 20471007 and 50972017).

References

[1] T. Thongtema, C. Pilaponga, S. Thongtemb, J. Alloys Compd. 496 (2010) L29–L32.
[2] L.Z. Cao, H. Jiang, H. Song, Z.M. Li, G. Miao, J. Alloys Compd. 489 (2010) 562.
[3] Z.Y. Ma, D. Dosev, M. Nichkova, R.K. Dumas, S.J. Gee, B.D. Hammock, K. Liu, I.M. Kennedy, J. Magn. Magn. Mater. 321 (2009) 1368.
[4] Y. Lu, C.L. Yan, S.Y. Gao, Appl. Surf. Sci. 255 (2009) 6061.
[5] H. Liu, G.X. Wang, D. Wexler, J.Z. Wang, H.K. Liu, Electrochem. Commun. 10 (2008) 165.
[6] L.Y. Li, Y.H. Cheng, X.G. Luo, H. Liu, G.H. Wen, R.K. Zheng, S.P. Ringer, Nanotechnology 21 (2010) 145705.
[7] H.B. Zeng, P.S. Liu, W.P. Cai, X.L. Cao, S.K. Yang, Cryst. Growth Des. 7 (2007) 1092.
[8] C.Y. Kuan, M.H. Hon, J.M. Chou, I.C. Leu, Cryst. Growth Des. 9 (2009) 813.
[9] D.M. Tang, G. Liu, F. Li, J. Tan, C. Liu, G.Q. Lu, H.M. Cheng, J. Phys. Chem. C 113 (2009) 11037.
[10] X.Y. Zhang, J.Y. Dai, C.H. Lam, H.T. Wang, P.A. Webley, Q. Li, H.C. Ong, Acta Mater. 55 (2007) 5039.
[11] W.Y. Chen, R.C. Wang, C.P. Liu, Cryst. Growth Des. 8 (2008) 2249.
[12] X.Y. Kong, Y. Ding, Z.L. Wang, J. Phys. Chem. B 108 (2004) 570.
[13] S.L. Wang, et al., J. Alloys Compd., 2010, doi:10.1016/j.jallcom.2010.04.042.
[14] S.C. Singh, R.K. Swarnkar, R. Gopal, Bull. Mater. Sci. 33 (2010) 21.
[15] M. Trejo, P. Santiago, H. Sobral, L. Rendon, U. Pal, Cryst. Growth Des. 9 (2009) 3024.
[16] X.L. Li, T.J. Lou, X.M. Sun, Y.D. Li, Inorg. Chem. 43 (2004) 5442.
[17] T. He, D.R. Chen, X.L. Jiao, Y.Y. Xu, Y.X. Gu, Langmuir 20 (2004) 8404.

[18] Y.D. Yin, Y. Lu, B. Gates, Y.N. Xia, Chem. Mater. 13 (2001) 1146.
[19] O. Lupan, L. Chow, G. Chai, H. Heinrich, Chem. Phys. Lett. 465 (2008) 249.
[20] Y. Zhang, W.F. Zhang, H.W. Zheng, Scripta Mater. 57 (2007) 313.
[21] K.M. Sulieman, X.T. Huang, J.P. Liu, M. Tang, Nanotechnology 17 (2006) 4950.
[22] M.H. Huang, Y.Y. Wu, H. Feick, N. Tran, E. Weber, P.D. Yang, Adv. Mater. 13 (2001) 113.
[23] J.Y. Lao, J.Y. Huang, D.Z. Wang, Z.F. Ren, Nano Lett. 2 (2003) 235.
[24] W. Ouyang, J. Zhu, Mater. Lett. 62 (2008) 2557.
[25] S. Braun, H.G. Grimmeiss, J. Appl. Phys. 45 (1974) 2658.
[26] A. Khan, W.M. Jadwisienczak, H.J. Lozykowski, M.E. Kordesch, Physica E 39 (2007) 258.
[27] W.S. Khan, C. Cao, Z. Chen, G. Nabi, Mater. Chem. Phys. 2010, in press, doi:10.1016/j.matchemphys.2010.06.072.
[28] F. Zong, H. Ma, C. Xue, H. Zhuang, X. Zhang, H. Xiao, J. Ma, F. Ji, Solid State Commun. 132 (2004) 521.
[29] G. Paniconi, Z. Stoeva, R.I. Smith, P.C. Dippo, B.L. Gallagherd, D.H. Gregory, J. Solid State Chem. 181 (2008) 158.
[30] A. Umar, Y.B. Hahn, Appl. Surf. Sci. 254 (2008) 3339.
[31] W.S. Khan, C. Cao, Appl. Phys. A: Mater. Sci. Process., in press.
[32] M.K. Lee, H.F. Tu, Cryst. Growth Des. 8 (2008) 1785.
[33] M. Kaur, S. Bhattacharya, M. Roy, S.K. Deshpande, P. Sharma, S.K. Gupta, J.Y. Yakhmi, Appl. Phys. A 87 (2007) 91.
[34] K.H. Liu, C.C. Lin, S.Y. Chen, Cryst. Growth Des. 5 (2005) 483.
[35] Y. Matsushima, M. Matsumoto, K. Maeda, T. Suzuki, Mater. Sci. Eng. B 145 (2007) 1.
[36] A. Ghosh, R.N.P. Choudhary, Phys. Status Solidi A 3 (2009) 206.
[37] D.H. Zhang, Z.Y. Xue, Q.P. Wang, J. Phys. D: Appl. Phys. 35 (2002) 2837.
[38] W. Liu, S.L. Gu, J.D. Ye, S.M. Zhu, S.M. Liu, X. Zhou, R. Zhang, Y. Shi, Y.D. Zheng, Y. Hang, C.L. Zhang, Appl. Phys. Lett. 88 (2006) 092101.
[39] Y.M. Sun, Ph.D. thesis, University of Science and Technology of China, July 2000 (16. Y. L).
[40] S.B. Zhang, S.H. Wei, A. Zunger, Phys. Rev. B 63 (2001) 075205.